

NRL Report 8152

Technique for Calibrating High Energy Laser Calorimeters

F. R. FLUHR, R. BERNARD BROWN, and GEORGE L. HALL

*High Energy Laser Facility
Optical Sciences Division*

October 11, 1977



NAVAL RESEARCH LABORATORY
Washington, D.C.

Approved for public release; distribution unlimited.

SECURITY CLASSIFICATION OF THIS PAGE (When Data Entered)

REPORT DOCUMENTATION PAGE		READ INSTRUCTIONS BEFORE COMPLETING FORM
1. REPORT NUMBER NRL Report 8152	2. GOVT ACCESSION NO.	3. RECIPIENT'S CATALOG NUMBER
4. TITLE (and Subtitle) TECHNIQUE FOR CALIBRATING HIGH ENERGY LASER CALORIMETERS		5. TYPE OF REPORT & PERIOD COVERED Final report on one phase of a continuing NRL Problem
		6. PERFORMING ORG. REPORT NUMBER
7. AUTHOR(s) F. R. Fluhr, R. Bernard Brown, and George L. Hall		8. CONTRACT OR GRANT NUMBER(s)
9. PERFORMING ORGANIZATION NAME AND ADDRESS Naval Research Laboratory Washington, D.C. 20375		10. PROGRAM ELEMENT, PROJECT, TASK AREA & WORK UNIT NUMBERS NRL Problem R05-31S Project SR03900182
11. CONTROLLING OFFICE NAME AND ADDRESS Department of the Navy Naval Sea Systems Command Washington, D.C. 20362		12. REPORT DATE October 11, 1977
		13. NUMBER OF PAGES 25
14. MONITORING AGENCY NAME & ADDRESS (if different from Controlling Office)		15. SECURITY CLASS. (of this report) Unclassified
		15a. DECLASSIFICATION/DOWNGRADING SCHEDULE
16. DISTRIBUTION STATEMENT (of this Report) Approved for public release; distribution unlimited.		
17. DISTRIBUTION STATEMENT (of the abstract entered in Block 20, if different from Report)		
18. SUPPLEMENTARY NOTES		
19. KEY WORDS (Continue on reverse side if necessary and identify by block number) Calorimeter Calorimeter design High-power laser Laser High energy laser		
20. ABSTRACT (Continue on reverse side if necessary and identify by block number) The technique uses high-power electric lamps to inject radiant energy into the calorimeter. With this technique, an NRL ball calorimeter was calibrated using 6 lamps emitting approximately 40 kW of power. Calorimeter constants are derived from measurements of the power to the lamps and the time duration. Factors affecting accuracy are described and accuracy of the technique is evaluated. Equations of predicted response are derived, and predicted values of response are compared to measured		

(Continued)

20. Continued

values. Methods used to minimize ambient temperature drift and to check calibration accuracy are described.

CONTENTS

I. INTRODUCTION	1
II. DESCRIPTION OF HIGH-POWER LAMP AND METERING CIRCUIT	3
III. BASIC CALORIMETER SHELL CALIBRATION WITH HIGH-POWER LAMP	4
Correction for Lamp Absorption	4
Results of Basic Shell Calibration	5
Linearity Determinations—Predicted vs Measured Response .	8
IV. FINAL CORRECTION FOR SCATTERING LOSS AND MIRROR ABSORPTION	8
V. CONCLUSIONS	12
APPENDIX A—Measurement of Scattering Loss	14
APPENDIX B—Correction of Previous Calorimeter Data	16
APPENDIX C—Calculation of Predicted Response	17
APPENDIX D—Calorimeter Electronics	20

TECHNIQUE FOR CALIBRATING HIGH ENERGY LASER CALORIMETERS

I. INTRODUCTION

The only practical method of routinely measuring high energy CW laser beam power at the Optical Radiation Laboratory (ORL) has been calorimetry using large hollow metal spheres. These spheres contain about 16 kg of aluminum whose temperature can be monitored to determine the amount of energy absorbed. The beam enters through a hole in the sphere and strikes a convex metal mirror that spreads it over the absorbing interior surface. The temperature of the sphere is read out through a copper resistance wire uniformly distributed over the sphere. The energy absorbed by the calorimeter is nearly proportional to the change in resistance. Average power incident \bar{P} is then found by dividing the energy absorbed by the exposure time. In addition, if power is known to be steady and is incident for a time longer than the thermal response time* of the aluminum sphere, then power can also be read out by measuring the rate of increase in resistance. This quantity is labeled P (slope) in this report. A diagram of the calorimeter and typical output trace is shown in Fig. 1 and 2.

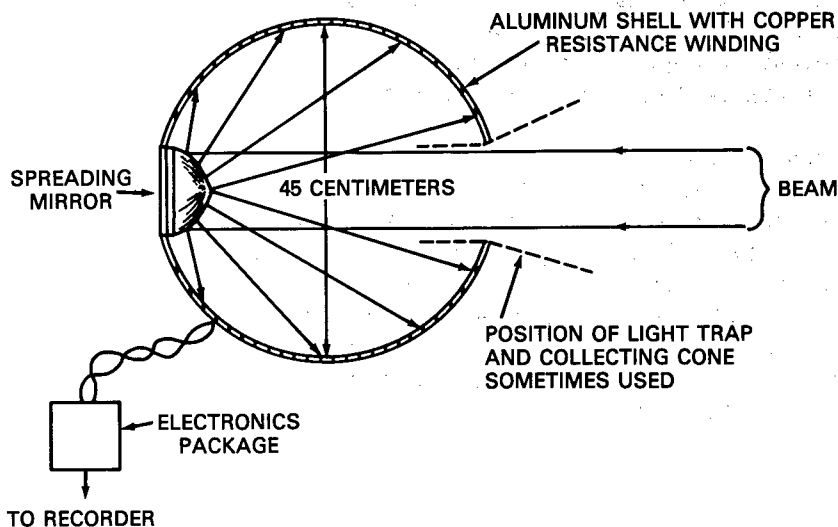


Fig. 1 — Spherical aluminum calorimeter (cutaway view)

*Thermal response time is the time required to reach steady state conditions; i.e., for a step function input, it is the time required for the temperature to begin changing linearly.

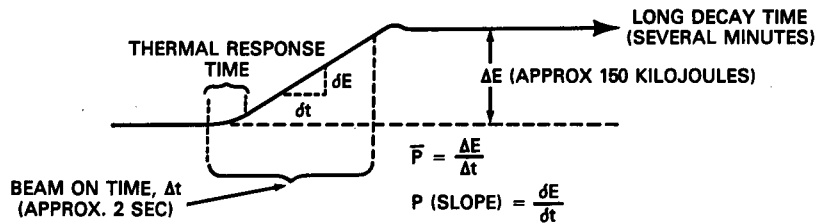


Fig. 2 — Typical recorder trace for constant input power

It was necessary to determine calibration coefficient Q for each calorimeter by measuring its temperature vs. resistance curve $\Delta T/\Delta R$, measuring the mass of aluminum M , and obtaining a handbook value for the heat capacity per unit mass C_m of the aluminum alloy. This gave the required coefficient as follows:

$$Q = \frac{\Delta E}{\Delta R} = \frac{\Delta E}{\Delta T} \frac{\Delta T}{\Delta R} = MC_m \frac{\Delta T}{\Delta R} \text{ KJ/ohm.}$$

One early method used to determine $\Delta T/\Delta R$ was to fill the sphere with water and heat the water with an electric immersion heater while stirring rapidly to obtain a uniform temperature. The curve was assumed to be linear from 20°C to 100°C, and a graphical average of measured values was used to calculate Q . Later, $\Delta T/\Delta R$ was calculated using a fixed initial value of temperature coefficient of resistance α and the initial measured value of resistance at 20°C. This method was found to be preferable to heating the calorimeter. Since this method also depended on a handbook value of C_m , it became desirable to devise an independent means of known accuracy to determine the value of Q .

A true calibration check requires that a known amount of energy be injected into the calorimeter shell and the response noted. This must be done in a short period of time compared to the cooling time of the sphere so that heat loss errors are negligible. Ideally, this can only be accomplished with a high-power, calibrated laser beam. The high-power lamp unit described in this report provides a simple means of approaching this ideal source. It provides significant amounts of radiant energy in a few seconds, which permits a true calibration. Furthermore, the energy is delivered in a steady, nearly square pulse, which permits the transient response characteristics of a particular calorimeter to be determined as well. This feature is important in the design work on rapid-response laser calorimeters and power meters.

The lamp calibration technique is less than ideal only in that the spreading mirror must be removed and the holes closed to prevent radiation loss during the basic calibration of the aluminum shell. This is necessary because of the broad radiation pattern of the lamp and the need to account for all of the lamp energy. After the basic calibration, the spreading mirror is replaced and a final correction is made as follows:

$$P(B) = P(E) + P(M) + P(S),$$

where $P(B)$ represents the power of a laser beam being measured, $P(E)$ is the power sensed by the calorimeter shell, $P(M)$ is the power absorbed by the spreading mirror, and $P(S)$ is the power scattered out through the input opening and lost.

II. DESCRIPTION OF HIGH-POWER LAMP AND METERING CIRCUIT

The lamp unit consists of a hollow brass tube that is mirror polished and gold plated on the outside to minimize absorption. The reflector accommodates up to 15 GE Q6M/T3/-CL/HT tungsten halogen lamps. The lamp unit is wired for a 3-phase delta supply of nominally 450 V. Each lamp produces about 6 kW, or slightly under 100 kW for all 15 lamps. Power input to the lamp stabilizes a few tenths of a second after turnon, and lamp warmup is nearly complete after 1 s. The extra energy absorbed by the lamp during warmup is small and is reradiated within a few seconds after the lamp is turned off. The calibration described in this report was done with 6 lamps operating at slightly under 40 kW. A photograph of the lamp assembly is shown in Fig. 3.

Power input to the lamp was monitored with a two-element polyphase wattmeter on loan from the Baltimore Gas and Electric Company (BG&EC). A diagram of the connection is shown in Fig. 4. External voltage multiplier resistors were required, and the sensing coils were in series, giving a scale multiplication factor of 8 as stated on the meter. Current transformers were also required to reduce current from the 50-A range to the 5-A range of the meter. This resulted in a further scale factor of $10 \times$ or a total of $80 \times$. A final correction for phase angle and loss as stated on the current transformers resulted in a net scale multiplication factor of 80.93. The voltage multiplier resistors were calibrated with the meter. The wattmeter was built to an accuracy of $\pm 0.5\%$ and was checked by BG&EC before being lent to NRL.

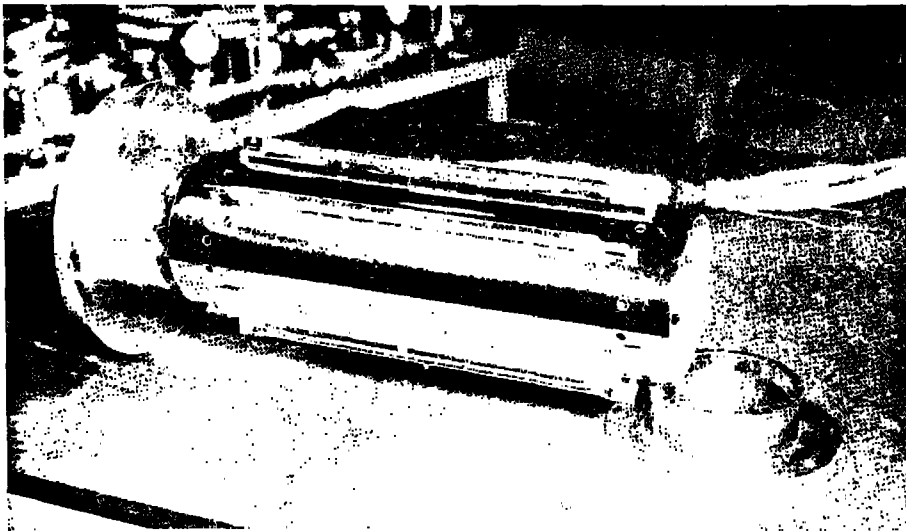


Fig. 3 — High-power lamp

FLUHR, BROWN, AND HALL

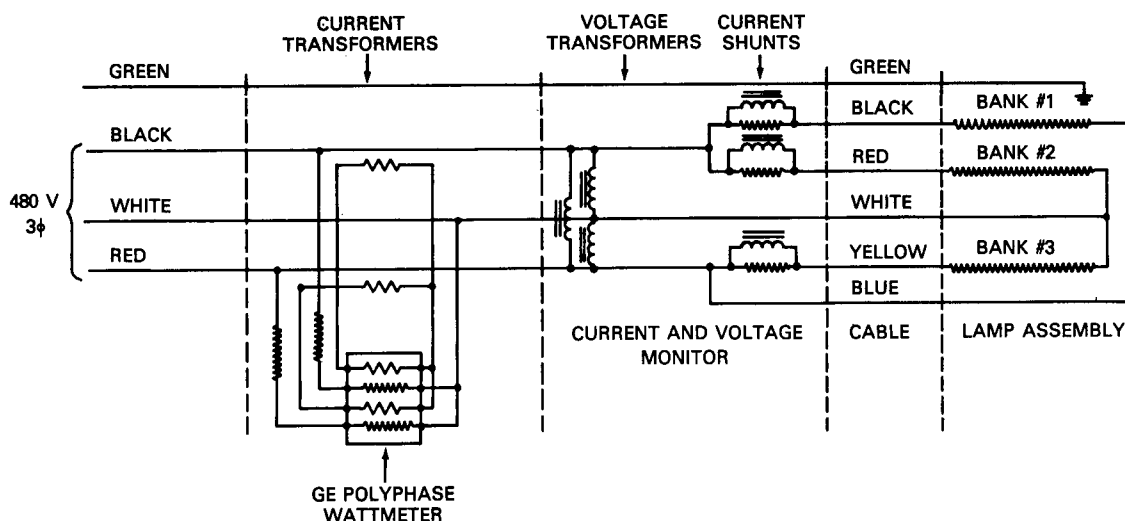


Fig. 4 — Wiring schematic of lamp and metering circuit

Individual voltages and currents obtained from additional shunts and transformers can be recorded during a run to detect line voltage changes or lamp changes. No changes were observed. The lamp power $P(E)$ is then $P(E) = \text{scale reading} \times 80.93 \text{ kW}$. The uncertainty is $\pm 0.2 \text{ kW}$. In the lamp unit, thermocouple outputs are also recorded in order to calculate the energy absorbed by the lamp reflector.

III. BASIC CALORIMETER SHELL CALIBRATION WITH HIGH-POWER LAMP

The two calorimeters on which the following tests were run were already in use at the Optical Radiation Laboratory, and calibration coefficient Q had been determined by the method described in the introduction. To carry out an independent determination of calibration coefficient Q , we devised the high-power lamp. The lamp unit was mounted in each calorimeter shell as shown in Fig. 5 and operated for a few seconds to give the desired energy input. The output of the calorimeter electronics package was recorded, together with current and voltage input information to the lamp, on a Honeywell CRT visicorder. The "on" time of the lamp was determined from the time-calibrated traces. After applying a correction for energy absorbed by the lamp itself, the metered power and the power read out by the calorimeter electronics were compared. Electrical power input $P(E)$ was metered using equipment previously described and accurate to $\pm 0.5\%$ of the scale reading, or $\pm 200 \text{ W}$ at 40 kW . To facilitate accurate reading of the wattmeter, a photograph was taken as soon as the pointer came to rest. For the shorter 4-s runs, this was very nearly at the end of the run. Lamp power was always steady throughout the run, as determined by the steady current and voltage traces on the recorder.

Correction for Lamp Absorption

The lamp reflector is slightly shorter than the diameter of the ball calorimeters so that reflective extenders must be used to fill the space and keep radiation from escaping. The

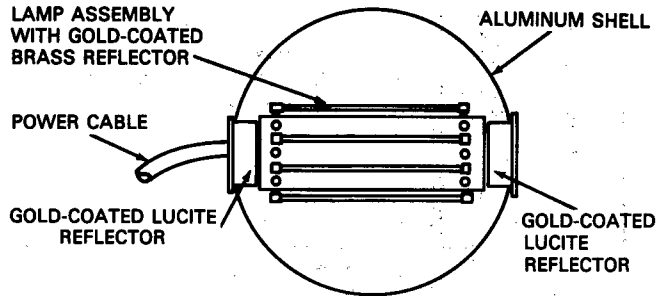


Fig. 5 - Lamp assembly installed in calorimeter shell

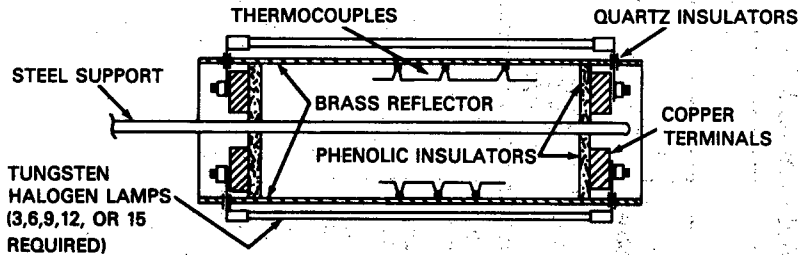


Fig. 6 - Cross section of lamp assembly

extenders are made of lucite covered with gold film. Their heat capacity and area are small, and radiation falling on them is not intense; no determination was made of the small amount of energy absorbed by them. The lamp reflector itself is large and receives nearly half the direct radiation from the lamps. Keeping accuracy high, requires a determination of the rate at which energy is absorbed by this reflector. Based on an absorptivity of 2% for gold, this reflector should absorb at a rate of at least 0.4 kW. When the lamp is installed in a calorimeter, thermocouples inside the reflector, as shown in Fig. 6, indicate that it absorbs at a rate of 1 kW. This value is uncertain by ± 0.25 kW (0.5%) because of the time constants associated with the measurement. Adjusted values of electrical power $P(E)$ are labeled $P(E)'$ in the tables, where

$$P(E)' = P(E) - 1 \text{ kW.}$$

Results of Basic Shell Calibration

The results of 23 runs on two calorimeters are given in Tables 1 and 2. Runs of various lengths were made, the shorter ones equivalent in energy input to a typical laser measurement and the longer ones taking the calorimeters to 0.5 mJ. Adjusted lamp power $P(E)'$ did not vary by more than 200 W from the mean during the 14 runs on calorimeter 1, nor more than 150 W on the 9 runs on calorimeter 2. The percent difference between these values and the values read out by the calorimeter electronics showed greater deviation. The mean

Table 1 — Lamp Power vs Calorimeter 1 Readout

		Lamp Power			Calorimeter Readout Power			
Run Number	Length of Run <i>t</i> (s)	Scale Reading <i>S</i>	Electrical Power <i>P</i> (<i>E</i>) (kW)	Adjusted Electrical Power <i>P</i> (<i>E</i>)' (kW)	Average Power \bar{P}	Percent Difference $\frac{P(E)' - \bar{P}}{P(E)'} \times 100$	Slope Power <i>P</i> (slope)	Percent Difference $\frac{P(E)' - P(\text{slope})}{P(E)'} \times 10$
1	4.74	490	39.7	38.7	36.3	6.2	36.3	6.2
2	4.85	491	39.7	38.7	37.5	3.1	35.8	7.5
3	4.42	488	39.5	38.5	36.4	5.5	35.3	8.3
4	4.31	490	39.7	38.7	36.4	5.9	35.3	8.8
5	4.11	490	39.7	38.7	36.3	6.2	35.1	9.3
6	5.14	490	39.7	38.7	36.2	6.5	34.9	9.8
7	4.86	489	39.6	38.6	35.6	7.8	35.2	8.8
8	3.82	488	39.5	38.5	35.6	7.5	35.0	9.1
9	6.11	489	39.6	38.6	36.0	6.7	35.6	7.8
10	6.80	489	39.5	38.5	36.2	6.0	34.7	9.9
11	9.50	491	39.7	38.7	36.3	6.2	35.3	8.8
12	11.75	492	39.8	38.8	35.5	8.5	35.1	9.5
13	12.05	490	39.6	38.6	36.1	6.5	35.7	7.5
14	12.12	488	39.5	38.5	35.9	6.8	35.3	8.3
				<38.6> $\sigma= .47\%$			<6.4> $\sigma=1.2\%$	<8.5> $\sigma=.98\%$

6

FLUHR, BROWN, AND HALL

Table 2 — Lamp Power vs Calorimeter 2 Readout

		Lamp Power			Calorimeter Readout Power			
Run Number	Length of Run <i>t</i> (s)	Scale Reading <i>S</i>	Electrical Power <i>P</i> (<i>E</i>) (kW)	Adjusted Electrical Power <i>P</i> (<i>E</i>)' (kW)	Average Power \bar{P}	Percent Difference $\frac{P(E)' - \bar{P}}{P(E)'} \times 100$	Slope Power <i>P</i> (slope)	Percent Difference $\frac{P(E)' - P(\text{slope})}{P(E)'} \times 10$
1	5.92	483	39.1	38.1	37.0	2.9	34.0	11.0
2	5.65	482	39.0	38.0	35.5	6.6	34.0	11.0
3	5.46	482	39.0	38.0	36.0	5.3	34.4	9.5
4	5.99	482	39.0	38.0	34.9	8.2	33.9	11.0
5	6.10	480	37.9	37.9	34.9	7.9	34.2	9.8
6	6.55	480	38.9	37.9	35.9	10.5	33.6	11.0
7	7.92	480	38.9	37.9	34.1	10.0	33.8	11.0
8	9.78	481	38.9	37.9	35.6	6.1	32.5	14.0
9	11.73	481	38.9	37.9	35.2	7.1	34.2	9.8
				<37.9> $\sigma = .43\%$			<7.2> $\sigma = 2.2\%$	<11> $\sigma = 1.3\%$

7

NRL REPORT 8152

readout of calorimeter 1, based on the original calibrations, was 6.4% low ($\sigma = 1.2\%$) for the average method and 8.5% low ($\sigma = 0.98\%$) for the slope method. The mean readout of calorimeter 2, based on the original calibration, was 7.2% low ($\sigma = 2.2\%$) for the average method and 11% low ($\sigma = 1.3\%$) for the slope method. Both the average and slope method values were calculated from the same output signal. The average method consists of determining an initial and a final value of the signal and dividing by the "on" time. This is done after the steep thermal gradient has leveled out and the output signal is steady.

The slope method consists of determining the rate at which the signal increases during the beam "on" time, when there is a thermal gradient present. Therefore, it is possible for the two methods to give slightly different values. The above results show that the average method corresponds more clearly to adjusted input power $P(E)'$ but that the slope method shows less scatter from run to run. One possible explanation for this is that the mechanics of measuring the slope introduces less error. Another is that the rate of temperature rise in the calorimeter may inherently be a more reliable way to extract the desired information. Therefore, once the calibration has been determined, the slope method would appear to be the more desirable readout method. Unfortunately, the slope method cannot be used regularly in practice because of the thermal time constants of these calorimeters, especially when the laser power is not steady.

Linearity Determinations—Predicted vs Measured Response

The predicted (theoretical) response of the calorimeters is essentially linear. Details of the calculations are given in Appendix C. Table C1 gives the results of the theoretical calculations for calorimeter 1 in terms of energy change vs resistance change out to 500 kJ. (If plotted graphically, it would appear perfectly linear.) When compared with a straight line intersecting at 500 kJ, the maximum deviation is slightly more than 1% and occurs in the vicinity of 50 kJ (about 297 K). This slight nonlinearity is mainly due to the variation in the handbook value of the heat capacity of the calorimeter's aluminum shell.

The measured response of both calorimeters is plotted in Figs. 7 and 8. Data points were taken from about 150 to 500 kJ using the high-power lamp. The deviation from linearity is slightly more than 3% for both calorimeters. Unfortunately, data were not taken in the 50-kJ range, where the predicted deviation was greatest.

In Fig. 9, data from both calorimeters are plotted in terms of energy input vs energy readout. The diagonal reference line represents an ideal calorimeter and shows graphically the deviation discussed in the last section.

FINAL CORRECTION FOR SCATTERING LOSS AND MIRROR ABSORPTION

As mentioned in the introduction, to use the calibrated shell as a laser beam calorimeter, two correction factors must be taken into account. The first is absorption by the spreading mirror, which was removed for calibration. Absorption by the spreading mirror $P(M)$, which is installed during normal operation and is thermally isolated from the calorimeter shell, represents power that is not measured by the calorimeter. The mirror is highly polished copper with a gold coating. The reflectivity of gold mirrors normally varies from

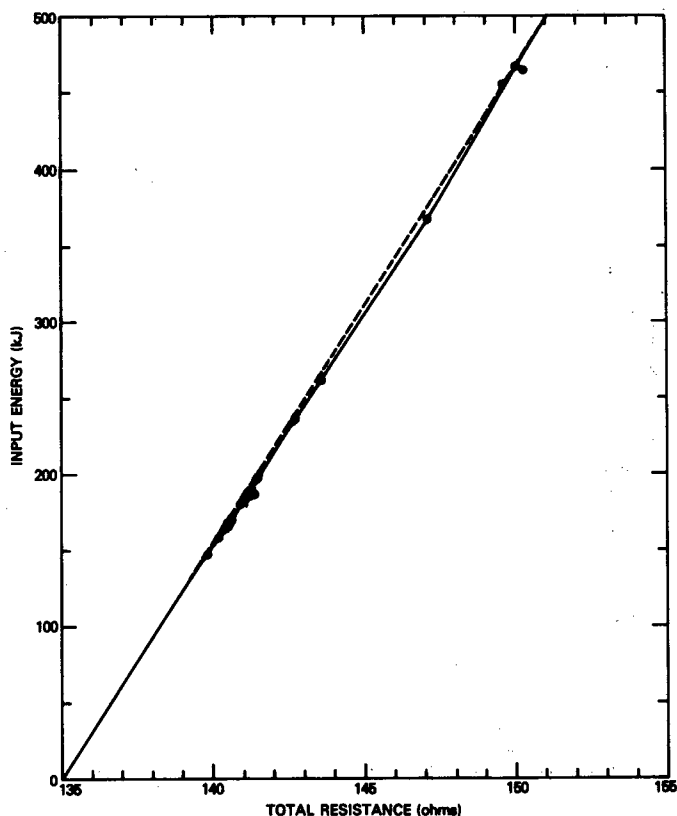


Fig. 7 — Measured input energy vs resistance for 14 runs on calorimeter 1. The straight reference line has been drawn to intersect the measured curve at 500 kJ. Maximum deviation from linearity is 10 kJ.

98 to 98.5%, but those used in the calorimeters have not been measured. Therefore, mirror absorption $P(M)$ is assumed to be $1.75 \pm 0.25\%$ of total beam power $P(B)$. The other factor affecting accuracy is scattering loss $P(S)$ out of the entrance port of the calorimeter. The first determination of this was made with thermally sensitive paper surrounding the entrance port during actual high energy laser runs. With the beam properly aligned on the spreading mirror, there was no darkening of the paper for 1-s runs. The threshold of the paper is about 1 W/cm^2 for a 1-s exposure. Following this, a small laser power meter was used to make measurements at various positions about the entrance port with a nominal 35-kW, 44-mm-diameter beam entering the calorimeter. The highest intensity observed during any run was 0.04 W/cm^2 at 67° from the input axis of the calorimeter. If this intensity existed over the whole hemisphere, it would total less than 200 W. Appendix A gives details of these measurements. Measurements of scattering loss in or near the main laser beam could not be made directly but were estimated from values of reverse amplified power* of typically 165 to 230 W from the input port of the Navy Tri-Service Laser (NTSL). These values also include contributions from three mirrors between the output window and calorimeter as well as laser cavity mirrors as shown in Fig. 10.

*This is reverse power that is amplified and exits through the input window of the high energy laser amplifier.

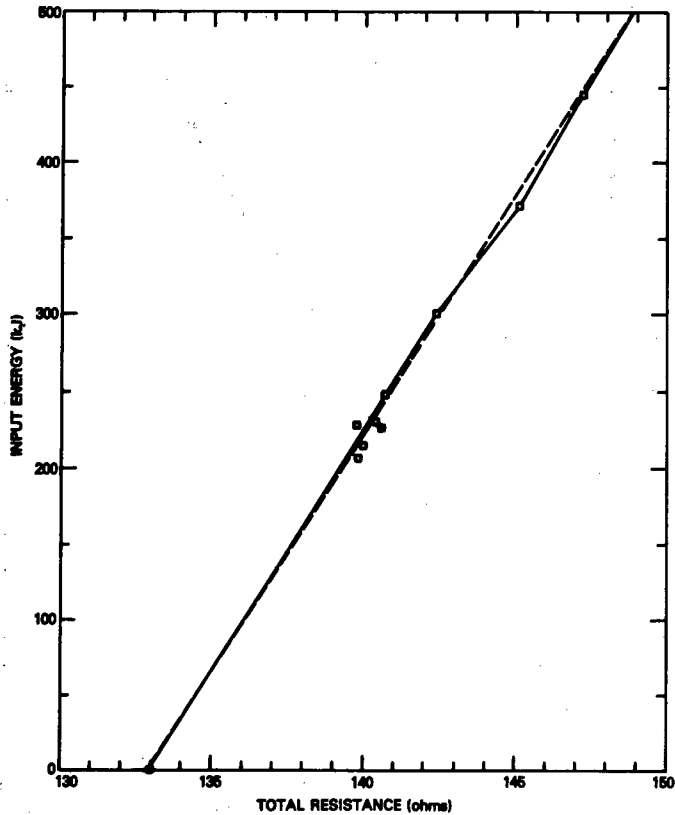


Fig. 8 — Measured input energy vs resistance for 9 runs on calorimeter 2. The straight reference line has been drawn to intersect the measured data at 500 kJ. Data is more scattered than for calorimeter 1 but deviation from linearity of the smoothed curve is only slightly greater.

If 1000 is used as the nominal high energy laser amplifier gain, the total effective backscatter is less than 1/4 W and the contribution of the calorimeter is a small part of that. This result is in agreement with the directly measured values previously mentioned. It indicates that scatter from the spherical calorimeters for a 100-kW, 44-mm beam is probably always less than 500 W. For larger beam diameters, the scattering loss can be expected to increase due to the geometry of the calorimeter, but this has not been measured. Accordingly, $P(S) = 0.25 \pm 0.25$ kW of total beam power $P(B)$.

When the above factors are taken into account for beam measurement purposes, total beam power $P(B)$ will be

$$P(B) = P(E)' + P(M) + P(S).$$

NRL REPORT 8152

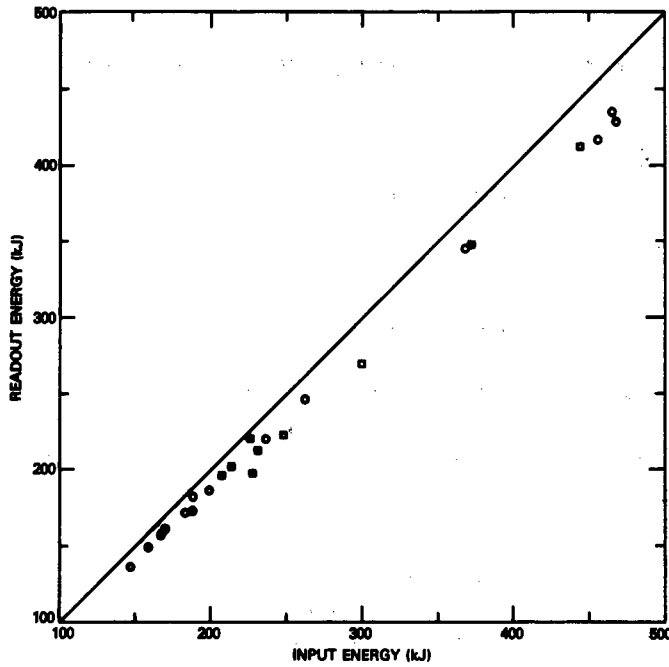


Fig. 9 — Readout vs input energy for both calorimeters. The diagonal straight line represents an ideal calorimeter under ideal conditions. The correction factors resulting from the lamp calibration have not been applied in this case. When they are applied, the data points are shifted upward and lie scattered about the diagonal line. Circles are for calorimeter 1 and squares are for calorimeter 2.

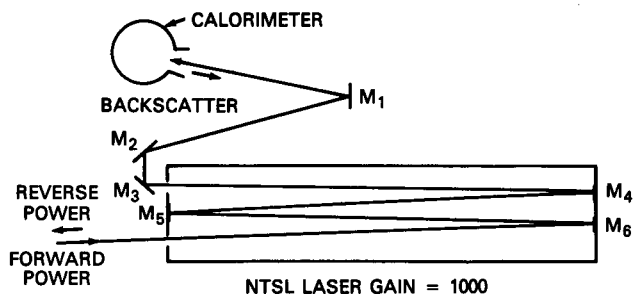


Fig. 10 — Drawing of optical train showing calorimeter and mirrors contributing to reverse amplified power. Measurement of the ratio of forward to reverse power gives an estimate of the upper limit of backscatter from the calorimeter.

FLUHR, BROWN, AND HALL

If we use

$$P(M) = 0.0175 P(B) \text{ and } P(S) = 0.0025 P(B),$$

then

$$P(B) = P(E)' + 0.02 P(B).$$

This reduces to

$$P(B) = 1.02 P(E)'.$$

That is, the actual beam power will be 2% higher than the basic electrical calibration.

A probable error in $P(B)$ will arise from the following independent factors:

Electrical power metering: $\pm 0.5\%$
Lamp absorption: $\pm 0.5\%$
Spreading mirror absorption: $\pm 0.25\%$
Scattering loss: $\pm 0.25\%$
Readout uncertainty*: $\pm 1.2-2.2\%$

The probable error is

$$[(0.5)^2 + (0.5)^2 + (0.25)^2 + (1.2)^2]^{0.5} = 1.4\% \text{ for cal. 1}$$

$$[(0.5)^2 + (0.5)^2 + (0.25)^2 + (2.2)^2]^{0.5} = 2.3\% \text{ for cal. 2,}$$

for the case of the averaging method of readout. This method is the one which was normally used, except for early runs when the two methods were averaged, or for certain runs when there was a malfunction. Since May 1975, a form of the average method has been used in the automated data reduction system put into operation at that time.

V. CONCLUSIONS

The electric lamp technique is a convenient and accurate way to check and calibrate high energy calorimeters. It should serve equally well for checking high energy power meters for laser beams when they are developed, provided the power meters have a design that permits inserting the lamp assembly. Since the measurements discussed in this report were made, a wattmeter was purchased for use with the lamp assembly. It does not require dropping resistors for the voltage coils but does require current transformers. A thermopile arrangement has also been installed in the lamp reflector to measure absorbed power more quickly and accurately. A digital temperature readout was also provided. The new wattmeter is of the moving coil type and still must be read or photographed.

*This uncertainty is the standard deviation of the data for \bar{P} in tables 1 and 2. It includes human mechanical error in data reduction, recorder error, and other electronic error.

The results of high-power lamp measurements made on ORL calorimeters 1 and 2, using previously determined calibrations, show that both were reading low at that time. Scatter in the data from calorimeter 2 indicated that there may have been an electrical defect such as a small intermittent resistance due to the switch in the calibrate circuit.

The measurement of power scattered from the calorimeter entrance aperture (Appendix A) indicates that scattering loss is low, less than 500 W for a 100-kW beam. Power scattered into the incoming beam could not be measured directly but was mentioned indirectly by observing the reverse-amplified power at the input to the NTSL amplifier. The low values observed were consistent with the low values measured directly at other angles.

The results of the high-power lamp measurements show that these calorimeters deviate from linearity by about 3% over the range 150 to 500 kJ. The results of calculations (Appendix C), using handbook values for the resistivity of copper wire and the heat capacity of pure aluminum, predict a deviation from linearity of about 1% from 0 to 500 kJ. This small disagreement is thought to be due mainly to the handbook values of heat capacity that were used—the actual composition of the aluminum alloy used in the calorimeters is unknown.

Appendix D discusses developments in the electrical operation and readout circuitry at the Optical Radiation Laboratory. This circuitry provides for referencing each run to the value of a stable, precision resistance and provides automatic zeroing and freedom from drift.

Appendix A

MEASUREMENT OF SCATTERING LOSS

The first attempt to measure scattering loss from the spherical calorimeters was to place thermally sensitive paper at the position of the dotted line in Fig. A1. The sensitivity of this paper was about 1 W/cm^2 for a 1-s exposure. There was no indication of scattering loss by the paper method. The second attempt was by means of the small power meter as shown in Fig. A1. This method resulted in the data given in Table A1. The highest intensity recorded was for run 1140. This intensity was calculated as follows:

$$I = \frac{1.7 \times 0.0612}{2.5} = 0.04 \text{ W/cm}^2.$$

If this intensity were to extend over the whole hemisphere indicated by the dotted line in Fig. A1, the scattering loss would be 162 W.

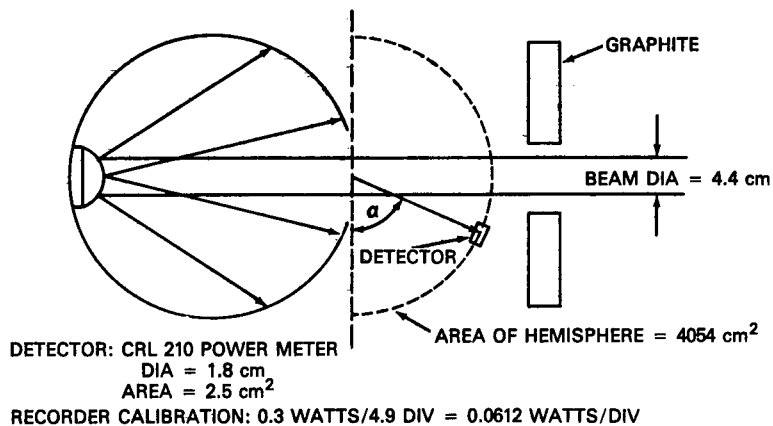


Fig. A1 — Arrangement used for measuring scattering Loss

Table A1

Run No.	Beam Power (kW)	α (deg)	Recorder Divisions
1136	37	45	1.0
1137	36	22	0.7
1138	35	10	0.2
1139	30	67	1.0
1140	36	67	1.7
1141	30	67	1.0
1143	32	67	1.0
1144	33	67	1.5
1145	36	67	0.6
1146	36	67	0.2
1147	33	67	1.0
1148	33	75	0.7
1149	26	75	0

Appendix B

CORRECTION OF PREVIOUS CALORIMETER DATA

Beginning with run 949 in February 1975, the following *basic* calibration was taken into account in the power readings quoted for the NRL calorimeters. If desired, data taken previously with these calorimeters may be corrected as follows.

Calorimeter 1; the basic calibration was low by 6.4% with an uncertainty of $\sigma = \pm 1.2\%$. It is low by another 2% due to mirror absorption and scatter loss. Therefore,

$$\text{correct value} = 1.02 \times 1.064 \times \text{old value.}$$

This 8.5% correction is uncertain by $\pm 1.4\%$ (probable error).

Calorimeter 2; the basic calibration was low by 7.2% with an uncertainty of 2.2%. It is low by another 2% due to mirror absorption and scattering loss. Therefore,

$$\text{correct value} = 1.02 \times 1.072 \times \text{old value.}$$

This 10% correction is uncertain by $\pm 2.8\%$ (probable error).

Appendix C

CALCULATION OF PREDICTED RESPONSE

To determine the predicted (theoretical) response of the calorimeter, it is necessary to know how heat capacity per unit mass C_m and winding resistance R vary with temperature in order to determine the form of calibration coefficient Q as a function of temperature, where

$$Q = M C_m \frac{\Delta T}{\Delta R} \quad \text{and} \quad \Delta E = Q \Delta R. \quad (\text{C1})$$

The mass of the calorimeter M is constant. Heat capacity per unit mass C_m does vary with temperature, as shown in the following reference values: $C(-50^\circ\text{C}) = 0.1914$ cal/g, $C(20^\circ\text{C}) = 0.214$ cal/g, $C(100^\circ\text{C}) = 0.225$ cal/g, $C(300^\circ\text{C}) = 0.248$ cal/g.* These values give the following four-point curve fit for C_m :

$$C_m = -4.1788 (10^{-2}) + 1.8115 (10^{-3}) T - 4.1703 (10^{-6}) T^2 + 3.3010 (10^{-9}) T^3 \text{ cal/K}. \quad (\text{C2})$$

This series may be integrated between any two temperatures in the range to give energy difference ΔE :

$$\Delta E = E(T_2) - E(T_1) = 4.1840M \int_{T_1}^{T_2} C_m dT \text{ kJ}, \quad (\text{C3})$$

where M is the mass of the calorimeter in kilograms and temperature is in kelvins.

The result for calorimeter 1 is

$$\Delta E = -2.8517 (T_2 - T_1) + 6.1809 (10^{-2}) (T_2^2 - T_1^2) - 9.4862 (10^{-5}) (T_2^3 - T_1^3) + 56316 (10^{-8}) (T_2^4 - T_1^4) \text{ kJ}. \quad (\text{C4})$$

This expression is the predicted variation of energy with temperature for calorimeter 1 and deviates from linearity a maximum of 0.7% from 0 to 500 kJ (293 to 327 K).

*From *Handbook of Chemistry and Physics*, 36th ed., Chemical Rubber Publishing Co., Cleveland (1954), p. 2085.

FLUHR, BROWN, AND HALL

Resistance vs temperature is more linear than ΔE vs ΔT . Values of α (in ohms/ohm-°C) the temperature coefficient of resistance for commercial copper are

$$\alpha(^{\circ}\text{C}) = 0.00427, \alpha(25^{\circ}\text{C}) = 0.003850, \alpha(50^{\circ}\text{C}) = 0.00352.*$$

The following curve may be fitted to these values, with temperature in kelvins:

$$\alpha(T) = \frac{1.3915}{T} - \frac{194.60}{T^2} + \frac{36298}{T^3}. \quad (\text{C5})$$

The exact relation between resistance and temperature is found by integrating the differential expression for α :

$$\alpha(\tau) = \frac{1}{R(T)} \frac{dR}{dT}$$

between two temperatures as follows:

$$\int_{R_1}^{R_2} \frac{dR}{R(T)} = \int_{T_1}^{T_2} \alpha(T) dT,$$

giving $\Delta R = R_2 - R_1 = R_1(e^B - 1)$

where

$$B = 1.3915 \ln \frac{T_2}{T_1} + 194.59 \left(\frac{1}{T_2} - \frac{1}{T_1} \right) - 18149 \left(\frac{1}{T_2^2} - \frac{1}{T_1^2} \right). \quad (\text{C6})$$

Values of ΔR calculated by this means may be compared to values calculated from the first order linear approximation to the above using the value of α at 0°C:

$$R_2 = R_1 [1 + 0.00427 (T_2 - T_1)]. \quad (\text{C7})$$

Values obtained from (C6) deviate from the linear approximation by no more than 0.03% over the range 0°C to 50°C. An exact calculation of ΔE vs ΔR using eqs. (C4) and (C6) gives a maximum deviation from linearity of slightly over 1% as shown in Table C1.

*H. Pendu, ed., *Electrical Engineers Handbook*, 4th ed., John Wiley & Sons, New York, sec. 2, p. 18. 1950

Table C1 — Predicted (Theoretical) Response of Calorimeter 1

R (ohms)	T (k)	$\frac{\Delta E}{(kJ)}$	ΔE (Linear Reference)	Percent Difference
135	293.00	0.0	0.0	0
136	294.89	27.6	27.9	1.1
137	296.77	55.2	55.9	1.3
138	298.66	82.9	83.8	1.1
139	300.55	110.6	111.8	1.0
140	302.44	138.4	139.7	0.9
141	304.32	166.2	167.7	0.9
142	306.21	194.1	195.6	0.8
143	308.09	222.0	223.6	0.7
144	309.98	250.0	251.5	0.6
145	311.87	277.9	279.5	0.6
146	313.75	306.0	307.4	0.5
147	315.64	334.0	335.3	0.4
148	317.52	362.1	363.3	0.3
149	319.41	390.2	391.2	0.3
150	321.29	418.4	419.2	0.2
151	323.17	446.6	447.1	0.1
152	325.05	474.8	475.1	0.1
153	326.94	503.0	503.0	0

The handbook values used in this calculation were given for pure aluminum and commercial copper. To improve on the above would require obtaining better data on the exact materials used in the calorimeter, i.e., #40 AWG copper magnet wire and the aluminum used to cast the shells. The aluminum composition was not specified and is not known. According to values of heat capacity for aluminum and its alloys, the values can vary depending on treatment and purity.* Nevertheless, it would require some extreme deviations in values to produce a significant change in the above result.

*See *Thermophysical Properties of High Temperature Solid Materials*, Y.S. Touloukian, ed., Macmillan Co., New York, 1967, vol. I, p. 11-12.

Appendix D

CALORIMETER ELECTRONICS

During the evolution of measuring high energy laser power, improved electronics were incorporated to minimize drift and maintain accurate calibration references.

To minimize readout drift due to changes in temperature of the laser calorimeter head, the electronics were zeroed when not in use. During this zeroing period, the circuit tracks drift due to ambient temperature changes and uses the final temperature value as a beginning point at the start of a calorimeter measurement. Since the measurement periods were short, on the order of 1s or less, the changes in energy measurement due to ambient temperature drift were negligible.

A calibrating technique that eliminates electronic, instrumentation, and recorder drift was incorporated into the calorimeter electronics. With the calibration constants derived for the calorimeter head, a standard change of resistance (ΔR_s) was determined, which was switched in series with the calorimeter head sensing resistor. This resistor was accurately adjusted to the value desired. It was a high-stability 0.1% low-temperature-coefficient resistor.

The value chosen for the calorimeters described in this report provided an equivalent 200-kJ change when switched in series with the calorimeter sensing resistance. This ΔR_s value was about 7 ohms for these nominal 135-ohm calorimeter sensing resistances. The exact value of ΔR_s was adjusted to two decimal places at the value required for the particular calorimeter head. The differences between calorimeter heads were primarily the differences in their masses.

The calorimeter electronics also include an analog differentiator that provided a signal proportional to the time rate of change of the energy signal in the calorimeter electronics. This provided an average power output signal during the period a calorimeter measurement occurred. The calibration of this output was indirectly related back to the standard ΔR_s resistor used to check the overall system calibration. A complete circuit schematic is shown in Fig. D1.

The basic sensing circuit consists of a constant-current generator (CCG) driving the sensing resistance in the calorimeter head. The sensing resistance consists of a #40 AWG copper wire wound in evenly spaced grooves cut in the spherical aluminum calorimeter head. In this case, the sensing resistance was about 135 ohms at room temperature. When the calorimeter temperature changes, the sensing resistance changes, thus causing a change of voltage drop across the sensing resistance. This voltage change is amplified to a value compatible with the associated recording instrumentation. In this case, the response factor is a nominal 1 V/100 kJ. This value does not have to be exact since the calibration is referenced to a 200-kJ change. The differentiator circuit gain was set to provide a response of about 1V/100 kW. Again exact values are not required. In normal operation, the energy and power calibration signals are activated just prior to a calorimeter measurement.

Immediately following the energy measurement, the calibration signals are again activated. This ensures that no major drifts or shifts occurred during calorimeter measurement.

As shown in Fig. D1, constant-current generator $Q1$ drives sensing resistance R_s . The current is nominally set at 5 mA. Calibration resistance ΔR_s is normally shorted by relay contacts $S2$. The voltage change caused by a change in R_s is amplified and buffered by operational amplifier $A1$. Amplifier $A2$ provides additional gain and drives drift-eliminating amplifier $A3$ and differentiating amplifier $A4$. Amplifier $A1$ provides the zeroing of the ambient temperature signals in order to keep the electronics in their linear operating regions. Amplifier $A2$ provides the desired gain scaling. Amplifier $A3$ is a very high-input impedance device. In the quiescent condition, relay contact $S1B$ connects the positive input of $A3$ to the negative input network. This allows capacitor C to charge to the ambient value of the system. Since the two inputs of amplifier $A3$ are connected to the same signal source, its output is zero. Also, the output of amplifier $A4$ is at 0 V DC since the drift changes are very slow. In operation, contact $S1B$ is opened, thus holding the positive input of $A3$ at the ambient value at the instant of contact opening. This allows amplifier $A3$ to amplify the calorimeter signal. During this same period, amplifier $A4$ differentiates the calorimeter signal, thus providing an output proportional to the average power being absorbed by the calorimeter head. At the end of the measurement, switch $S1B$ closes and the circuits reestablish the new ambient state. Capacitor C charges to a value corresponding to the new temperature of the calorimeter head, thus allowing additional calorimeter measurements without requiring the calorimeter head to cool back to the original temperature. This can be done so long as the sensing resistance and specific heat of the aluminum ball remain within their linear regions of operation.

To calibrate the energy response of the circuit, relays $S1$ and $S2$ are activated. This puts amplifier $A3$ in its active state and introduces ΔR_s resistance in series with sensing resistance R_s . A 200-kJ signal is then generated in the amplifier chain. The power calibration is accomplished by activating relays $S1$ and $S3$. $S3$ allows ramp generator $A5$ to introduce a sweep voltage on the sensing resistance network. This sweep voltage is adjusted to provide a 100-kJ/s signal into the amplifier chain. The energy \bar{E} output signal is a 100-kJ/s sweep and the power \bar{P} output is a DC voltage proportional to a 100-kW signal.

The calorimeter was set up to be operated manually or by remote control.